

## AGATES FROM GURASADA, SOUTHERN APUSENI MOUNTAINS, ROMANIA: AN XRD AND THERMOGRAVIMETRIC STUDY

Ciprian CONSTANTINA<sup>1</sup> & Terry MOXON<sup>2</sup>

<sup>1</sup>North University of Baia Mare, 62A Dr. V. Babes Street, 430083, Baia Mare, Romania, cconstantina@yahoo.com;

<sup>2</sup>55 Common Lane, Auckley, Doncaster, DN9 3HX, England

**Abstract** A suite of agates from Gurasada, Romania have been characterised using powder X-ray diffraction, thermogravimetry and density determinations. A comparison of agate data from Gurasada with 14 other world-wide regions reveals discrepancies in the Gurasada agate information. The crystallite size, density, defect-site water and moganite content demonstrate that these agates can be characteristically divided into two groups. One group reveals properties that are consistent with a contemporaneous formation around the age of the ~75Ma old host. Host rock bentonitisation is a likely silica source for the second group of agates that have apparently formed ~ 55 Ma later. Additionally, a number of the Gurasada agates contain cristobalite that exists as a white rind and within the agate structure.

**Key words:** Apuseni Mountains, Cretaceous, Neogene, agate, cristobalite, chalcedony, XRD

### 1. INTRODUCTION

Chalcedony is a group name for the compact varieties of silica mainly composed of minute crystals of  $\alpha$ -quartz with submicroscopic pores. The colour and texture may vary considerably, but in general such materials may be subdivided into chalcedony where the colour is fairly uniform and agate where the colour is arranged in bands (Deer et al. 1992). Sectioned agates often reveal wall-lining banding as a series of distorted onion-like rings and, under the polarizing microscope, agate and chalcedony generally show a fibrous structure. Agates are most frequently found in fine-grained igneous rocks filling gas vesicles, but can also be found in some sedimentary hosts e.g. Minnelusa Formation, South Dakota, USA (Clark, 2009); Phosphoria Formation, Montana, USA (Götze et al., 2009), and fossil wood (Daniels & Dayvault, 2006).

In spite of the world-wide occurrence of agate, its genesis continues to be an on-going enigma. Aspects that still require an explanation include the silica source, method of silica transportation and the manner of crystallization that results in the remarkable repetitive banding. Likely origins would be either the direct formation of chalcedony or the deposition of amorphous silica, gel or powder,

which then evolves into chalcedony. The formation temperature now has a consensus: most recent workers agree that agates form at temperatures < 100°C (Heaney, 1993). Agate sometimes contains a hidden co-deposit of calcite together with  $\alpha$ -quartz but more usually it has a very high silica content (> 97%) with non-volatile impurities being < 1% (Flörke et al. 1982). The total water as free (H<sub>2</sub>O) and silanol (Si—OH) is the major impurity in agate with concentrations up to ~2% (Graetsch et al. 1985). Mineral phase identification in agate is generally limited to a mixture of the two silica polymorphs: moganite and  $\alpha$ -quartz.

Recent studies on agate and chalcedony from a variety of hosts aged 13 to ~ 60 Ma demonstrated host-age related properties with a general decrease in moganite content and defect-site water, but an increase in crystallite size and density with increasing age. The same properties of agates from hosts aged from ~ 400 to 1100 Ma were shown to be approximately constant (Moxon & Ríos, 2004, Moxon et al. 2006). A later study allowed a further refinement of the data and additionally demonstrated that various stages of crystallite development were essentially the result of a transformation of moganite to  $\alpha$ -quartz (Moxon & Carpenter, 2009).

The prime objective of the present study was to characterise the agates from Gurasada, Romania and relate the new data to previously determined agate age-related properties of crystallite size, moganite content, defect-site water and density. Throughout the paper, the numbers in parentheses are  $\pm$  one standard deviation.

## 2. REGION, SAMPLES AND METHODS

### 2.1 Gurasada region and agate samples

Gurasada is located south of the Apuseni Mountains, about 20 km west from the Deva municipality. The hilly landscape is cross-cut by a network of north-south oriented valleys that are

tributaries of the River Mureş. Here, the agate and chalcedony host-rock is andesitic pyroclastic breccia. These rocks have been emplaced via sub-aerial volcanic effusive activity associated with the Laramian magmatism (Upper Cretaceous–Paleocene). Radiometric measurements for these rocks have a determined age of 69–80 Ma (Constantina et al. 2009), and for this paper a host rock age of 75 Ma will be used. The pyroclastic breccia is most frequently strongly altered (bentonitised). The volcanic rocks are in contact with calcareous sedimentary deposits (Lower Cretaceous) and Mesozoic ophiolitic rocks of basaltic composition (Jurassic). In addition, Quaternary deposits are also present along the main river beds (Fig. 1).

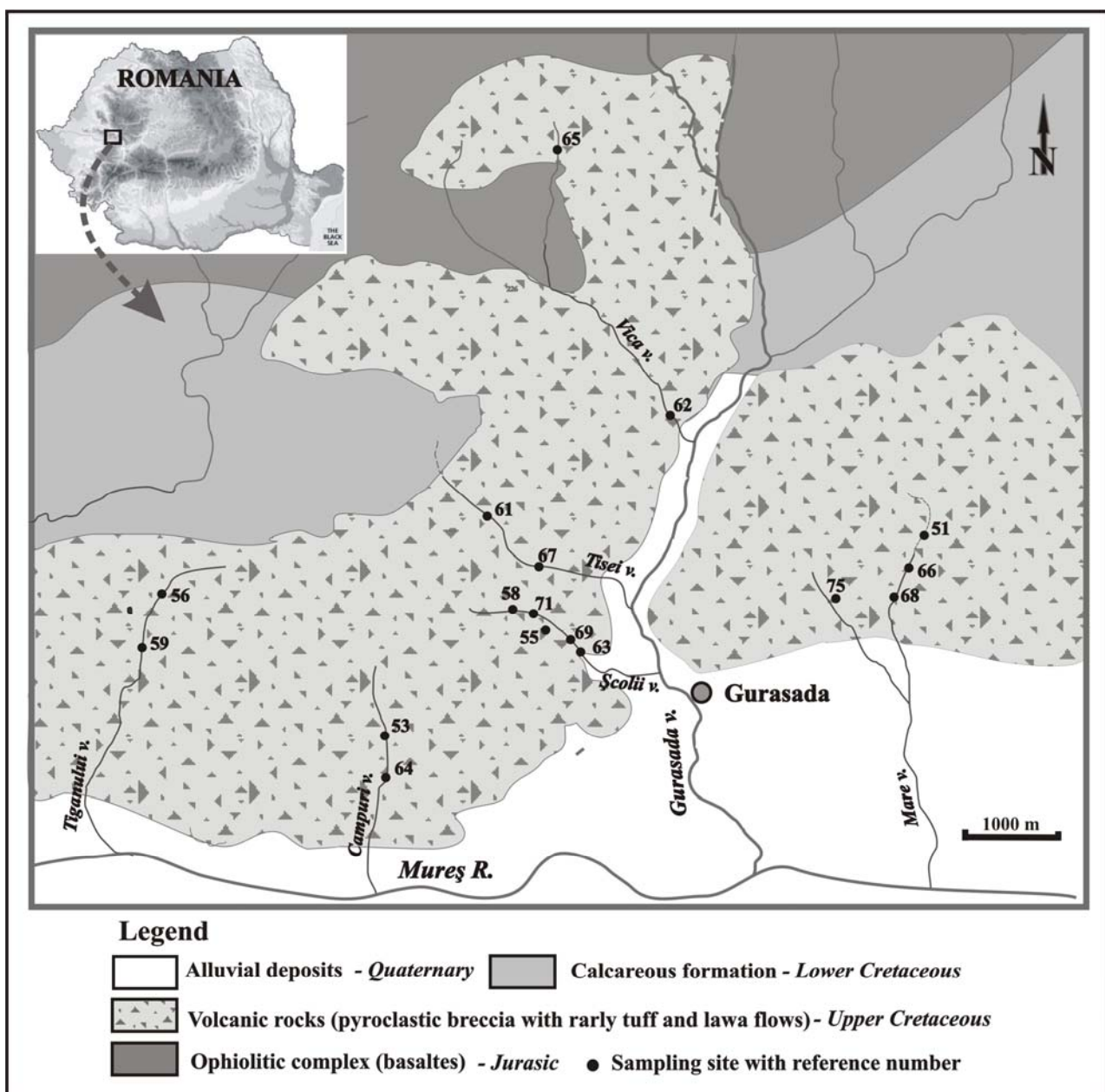


Figure 1. Simplified geological map of the Gurasada region.

The present study is limited to an examination of agate and chalcedony associated with pyroclastic breccias. However, other siliceous deposits of jasper, opal and silicified wood can also be found in this area. Gurasada agates are of the wall-lining type and they usually display light colours with a typical core of milky-white  $\alpha$ -quartz. Multicoloured agates with a red outer rim and greyish-blue inner have also been recorded. Chalcedony is generally found within

nodules or veins showing dominant white to grey-blue or brown hues. The size of the chalcedony nodules varies from a few cm up to 0.5-0.7 metres in diameter. Evidence of a later river working of the samples is demonstrated by the quasi-rounded shapes. The present study has examined 17 Gurasada samples with numbers 55 and 75 collected *in situ* while the remainder have been found in valley alluvia (Fig. 2 and Table 1).

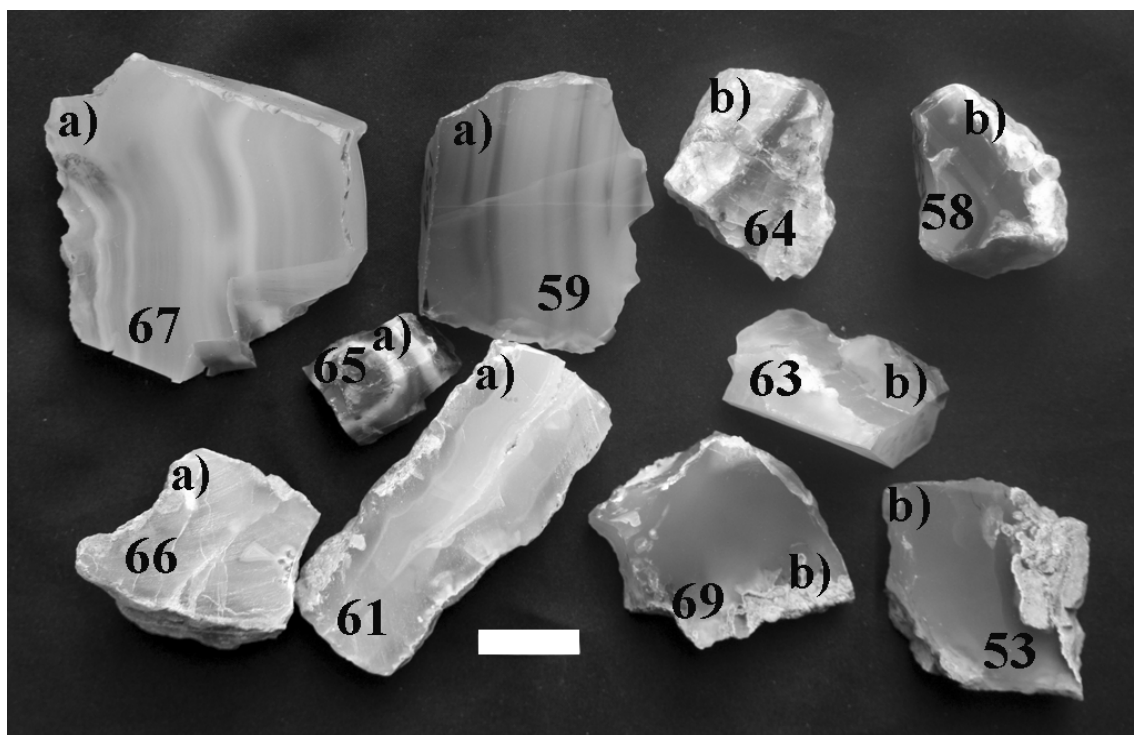


Figure 2. Representative samples of agate and chalcedony from the Gurasada region. The collection has been characterised into two groups showing a) high crystallite size and b) low crystallite size. Scale bar = 2 cm.

Table 1. Agate samples used for: <sup>x</sup> –XRD, <sup>y</sup>-TGA

Region	Site and sample number	Collector
<i>Reference agates</i>		
1. Yucca Mt. USA	Yucca Mt. HD2257 <sup>x</sup>	(LN)
2. Mt. Warning, Australia	Oxley River, Queensland 1 <sup>xy</sup> , 2 <sup>xy</sup> , 3 <sup>xy</sup> , 4 <sup>xy</sup> , 5 <sup>xy</sup> , 6 <sup>xy</sup> , 7 <sup>x</sup> , 10 <sup>xy</sup> , 12 <sup>xy</sup>	(JRi)
3. Texas, USA	Cottonwood Springs 1 <sup>x</sup> , 2 <sup>x</sup> , 4 <sup>x</sup> , 5 <sup>x</sup> , 6 <sup>x</sup> , 7 <sup>x</sup>	(BC)
4. Chihuahua, Mexico	Ojo Laguna 3 <sup>xy</sup> , 5 <sup>xy</sup> , 7 <sup>y</sup> , 9 <sup>xy</sup> , 10 <sup>xy</sup> , 11 <sup>xy</sup> , 12 <sup>xy</sup> , 14 <sup>x</sup> , 15 <sup>x</sup>	(BC)
5. Washington, USA	Ellensburg 1 <sup>xy</sup> , 2 <sup>xy</sup> , 3 <sup>xy</sup> , 4 <sup>xy</sup> , 5 <sup>xy</sup> , 6 <sup>xy</sup>	(PH)
6. Las Choyas, Mexico	Las Choyas 1 <sup>xy</sup> , 2 <sup>xy</sup> , 3 <sup>xy</sup> , 4 <sup>xy</sup> , 5 <sup>xy</sup> , 6 <sup>xy</sup>	(BC, JC)
7. Khur, Iran	Khur 2 <sup>y</sup> , 5 <sup>x</sup> , 7 <sup>x</sup> , 10 <sup>y</sup> , 23 <sup>y</sup> , 24 <sup>xy</sup> , 31 <sup>x</sup> , 33 <sup>xy</sup> , 48 <sup>x</sup> , 50 <sup>xy</sup> , 65 <sup>xy</sup>	(MN)
8. BTVP, Scotland	Mull 1 <sup>xy</sup> , 2 <sup>y</sup> , 5 <sup>y</sup> , 11 <sup>xy</sup> , Rum 2 <sup>y</sup> , 12 <sup>xy</sup> , 15 <sup>xy</sup> , 17 <sup>y</sup> , 19 <sup>xy</sup>	(RL, BT)
9. Canterbury, New Zealand	Mt. Somers 1 <sup>x</sup> , 2 <sup>x</sup> , 4 <sup>x</sup> , 14 <sup>x</sup> , 17 <sup>x</sup> , 20 <sup>x</sup> , 21 <sup>a</sup> , 24 <sup>x</sup>	(RB, VT)
10. Rio do Sul, Brazil	Soledado Mines 9 <sup>x</sup> , 20 <sup>x</sup> , 21 <sup>x</sup> , 26 <sup>x</sup> , 37 <sup>x</sup> , 58 <sup>x</sup> , 60 <sup>x</sup> , 62 <sup>x</sup> , 64 <sup>x</sup>	(purchased)
11. Semolale, Botswana	Bobonong 20 <sup>x</sup> , 49 <sup>xy</sup> , 75 <sup>x</sup> , 77 <sup>xy</sup> , 79 <sup>xy</sup> , 80 <sup>xy</sup> , 85 <sup>x</sup> , 86 <sup>x</sup> , 95 <sup>y</sup> , 99 <sup>y</sup> , 110 <sup>x</sup>	(HK)
12. Nova Scotia, Canada	Bay of Fundy 2 <sup>x</sup> , 6 <sup>x</sup> , 7 <sup>y</sup> , 9 <sup>x</sup> , 12 <sup>x</sup> , 13 <sup>xy</sup> , 16 <sup>x</sup> , 18 <sup>xy</sup> , 19 <sup>y</sup> , 21 <sup>xy</sup> , 28 <sup>xy</sup>	(BI)
13. Queensland, Australia	Agate Creek 1 <sup>y</sup> , 2 <sup>xy</sup> , 4 <sup>y</sup> , 5 <sup>xy</sup> , 7 <sup>x</sup> , 12 <sup>x</sup> , 14 <sup>xy</sup> , 18 <sup>x</sup> , 22 <sup>x</sup> , 105 <sup>xy</sup> , 109 <sup>x</sup> , 114 <sup>x</sup> , 129 <sup>x</sup>	(NC)
14. Thuringia, Germany	Thuringia Forest 3 <sup>xy</sup> , 5 <sup>xy</sup> , 9 <sup>xy</sup> , 10 <sup>xy</sup> , 11 <sup>x</sup> , 14 <sup>xy</sup> . Idar 3 <sup>xy</sup>	(GH)
Gurasada agates	Gurasada 51 <sup>xy</sup> , 53 <sup>xy</sup> , 55 <sup>x</sup> , 56 <sup>x</sup> , 58 <sup>xy</sup> , 59 <sup>xy</sup> , 61 <sup>xy</sup> , 62 <sup>x</sup> , 63 <sup>xy</sup> , 64 <sup>xy</sup> , 65 <sup>xy</sup> , 66 <sup>x</sup> , 68 <sup>x</sup> , 67 <sup>xy</sup> , 69 <sup>xy</sup> , 71 <sup>x</sup> , 75 <sup>x</sup>	(CC)

The Gurasada agates have been compared with an agate data base that has been previously created using material from various world-wide sources. All these samples are from a range of igneous hosts aged from 13 to 285 Ma and, apart from three exceptions, the reference materials are wall-lining agates. Relatively young chalcedony found in igneous hosts from the Yucca Mountain, Nevada, USA (13 Ma), Mt Warning, Queensland, Australia (23 Ma) and Cottonwood Springs, Texas, USA (37 Ma) is also included (Table 1).

## 2.2 Experimental Methods

*X-ray diffraction (XRD).* Measurement of accurate powder XRD intensities requires a grain size of  $< 10 \mu\text{m}$  (Bish & Reynolds, 1989). A portion of each agate was first hand-ground and sieved to obtain grain sizes  $< 52 \mu\text{m}$ . A fixed mass of the sieved powder was mixed with ethanol and ball-mill ground to produce powders in the 4 to 10  $\mu\text{m}$  range. Diffraction patterns were obtained from these powders using a Bruker D8 diffractometer in reflection mode. Preliminary scans over the  $16^\circ < 2\theta < 80^\circ$  range provided initial identification of the mineral phases present.

Crystallite size ( $C_{s(101)}$ ) determinations were based on the main (101) quartz reflection at  $26.64^\circ 2\theta$ , as recorded in separate scans over the range  $17^\circ < 2\theta < 30^\circ$  with a step size of  $0.01^\circ 2\theta$  and a scan speed of 10 s/step. Silicon powder was added as an internal standard for instrument broadening corrections.

The crystallite sizes are based on the mean crystallite size ( $C_{s(101)}$ ) that is taken to be representative of the mean crystallite diameter. This thickness perpendicular to the (101) plane has been calculated using the Scherrer equation:

$$C_{s(101)} = \frac{K\lambda}{\cos \theta \sqrt{\beta_q^2 - \beta_s^2}} \quad (1)$$

The full width at half maximum of the (101) peak was measured along with FWHM of Si at  $28.44^\circ 2\theta$  ( $\beta_s$ ) for instrument broadening corrections. The shape factor  $K$ , was taken as unity and  $\lambda$  is the wavelength of  $\text{CuK}\alpha_1$  radiation. Extensive crushing and ball mill grinding negates an inclusion of strain broadening in equation (1).

Most agates contain moganite but the determination of low level moganite using Rietveld refinement is imprecise due to overlapping of the moganite and  $\alpha$ -quartz peaks. An alternative estimation of the moganite content was previously discussed, and this method has been used for the

present study (Moxon & Rios, 2004; Moxon & Carpenter, 2009). Diffraction patterns were collected over the range  $17^\circ < 2\theta < 25^\circ$  to include the strongest moganite peaks at  $\sim 20^\circ 2\theta$  and the (100)  $\alpha$ -quartz peak at  $20.84^\circ 2\theta$ , using a step size of  $0.02^\circ$  and a scan rate of 20 s/step. The moganite and  $\alpha$ -quartz peak areas were determined by fitting two unconstrained Lorentzian functions using the Advanced Fitting Tool in *OriginLab*; the total area was obtained using the baseline tool. Moganite content has been taken as the proportion (in %) of peak area moganite / total peak area, with an estimated resolution of  $\pm 2\%$ .

*Thermogravimetric Analysis (TGA)* A number of studies have investigated chalcedony and agate dehydration over the 20 to 1400°C temperature range; these investigations produced similar TGA dehydration curves (Graetsch et al. 1985; Petrovic et al. 1996; Yamagishi et al. 1997). Initially, there is a loss of loosely bound water and TGA plots show that this is complete at  $\sim 150^\circ\text{C}$  with minimal water loss up to  $\sim 200^\circ\text{C}$ . Tightly bound water and some silanol water (Si-OH) is slowly removed between 200 and  $\sim 400^\circ\text{C}$ , and followed by a rapid rate of water loss up to  $\sim 600^\circ\text{C}$ . Dehydration is complete with the loss of the remaining defect-site water (mainly silanol Si-OH) at temperatures of  $\sim 1000^\circ\text{C}$ .

For this study, agate samples were crushed and sieved to  $< 52 \mu\text{m}$ , and free molecular water was found by heating the powders in a box oven at  $170^\circ\text{C}$  for 4 hours. Total water was determined by furnace heating at  $1200^\circ\text{C}$  for 2 hours. These heating times were sufficient to produce a constant mass loss. Mass loss differences between total and free water give the defect-site water content. At least six agates were selected from each region and each run was carried out in triplicate. Post  $170^\circ\text{C}$  dehydration will be referred to as defect-site water loss throughout this paper.

*Density* The agate density data was determined by the method of hydrostatic weighing. However, some of the Gurasada samples contained interwoven extraneous material and only 10 of the 17 agates were suitable for density determination.

## 3. RESULTS

*Crystallite size and moganite content.* XRD scans of the 17 Gurasada agates showed that 10 samples contained moganite and  $\alpha$ -quartz only; the remaining seven samples contained either additional calcite or cristobalite. The overall mean crystallite size ( $C_{s(101)}$ ) obtained from 17 Gurasada samples produced a very high mean standard deviation of  $\pm 25\%$ ; this

compared with the  $\pm 9\%$  mean standard deviation of agates from seven agate regions found in hosts  $\leq 60$  Ma (Table 2). The Gurasada data in Table 2 is presented as an overall mean crystallite size for the 17 samples, and as two groups showing a crystallite size  $>$  or  $< 60$  nm. These two groups are designated as high and low crystallite size respectively. Previously determined agate data from hosts aged between 13 and 285 Ma are also given in Table 2.

Sample diffraction data fits to estimate the moganite content are shown in Fig. 3 and the moganite content for individual Gurasada samples is shown in table 3.

**Thermogravimetric Analysis** New defect-site water data is presented for agates found in Gurasada, Romania; Las Choyas, Mexico; Bobonong, Botswana and Bay of Fundy, Nova Scotia, Canada. All other data has been given elsewhere. The same study also showed that the mean free water in agate was independent of the age of the host rock (Moxon & Ríos, 2004). The mean free water found for the two Gurasada groups defined as high and low crystallite size is 0.12(0.06)% and 0.20(0.05)% respectively.

High temperature heating of samples containing either calcite or cristobalite was not investigated as these would produce an increased

non-quantifiable mass loss. The mean value of the defect-site water from the remaining 10 Gurasada samples is well off trend (point a) in Fig. 4 II. This Gurasada defect-site water data is also separately applied to the same two groups showing low and high crystallite size (points b and c respectively in Fig. 4 II).

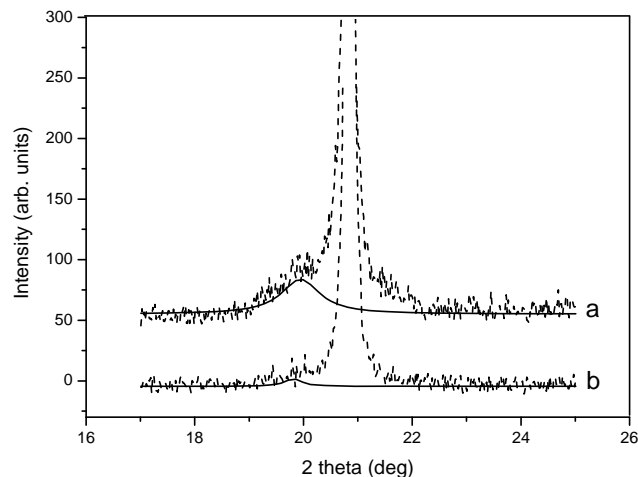


Figure 3 The original diffractograms are fitted with the moganite peaks at  $\sim 20^\circ 2\theta$  (solid line). The plots show the range of the moganite content in a) No. 53 with 19% moganite, b) No. 65 with 2% moganite. The plots were scaled to the same  $\alpha$ -quartz peak intensity.

Table 2. Variation of crystallite size and moganite content with the age of the host rock

<i>Region</i>	<i>Age of host (Ma)</i>	<i>No of samples</i>	<i>Mean Cs<sub>(101)</sub> /nm (<math>\pm\sigma</math>)</i>	<i>No of samples</i>	<i>Moganite /% (<math>\pm\sigma</math>)</i>
<i>Reference agates</i>					
1. Yucca Mt. USA	13c	1	40	1	56
2. Mt Warning, Queensland, Australia	23c	9	49(4)	7	19(4)
3 Cottonwood Springs, Texas, USA	37d	6	59(6)	6	10(4)
4. Chihuahua, Mexico	38d	9	57(4)	6	12(4)
5. Washington, USA	43d	6	68(6)	6	9(5)
6. Las Choyas, Mexico	45d	6	65(4)	4	9(5)
7. Khur, Iran	50a	8	79(11)	13	6(5)
8. BTVP, Scotland	60a	6	71(4)	6	11(2)
9. Mt Somers, Canterbury, N. Zealand	89e	8	56(5)	9	11(4)
10. Rio do Sul, Brazil	133a	9	52(7)	10	18(4)
11. Semolale, Botswana	180c	9	79(9)	8	3(2)
12. Nova Scotia, Canada	202d	8	71(9)	5	5(1)
13. Agate Creek, Queensl', Australia	275a	11	74(8)	7	6(2)
14. Thuringia, Germany	285a	7	83(4)	6	5(5)
15. Gurasada agates	75b				
Low Cs <sub>(101)</sub>		10	46(3)	9*	17(9)
High Cs <sub>(101)</sub>		7	71(7)	7	7(6)
Overall Cs <sub>(101)</sub>		17	56(14)	13	11(7)

Age reference given in: a Moxon (2002); b Constantina et al., (2009); c Moxon et al., (2006); d Moxon & Carpenter (2009). XRD data for Regions 1 to 14, after Moxon & Carpenter (2009).

\*One sample contained a high cristobalite content preventing an accurate moganite determination.

Regions in italics are considered as outliers: see text.

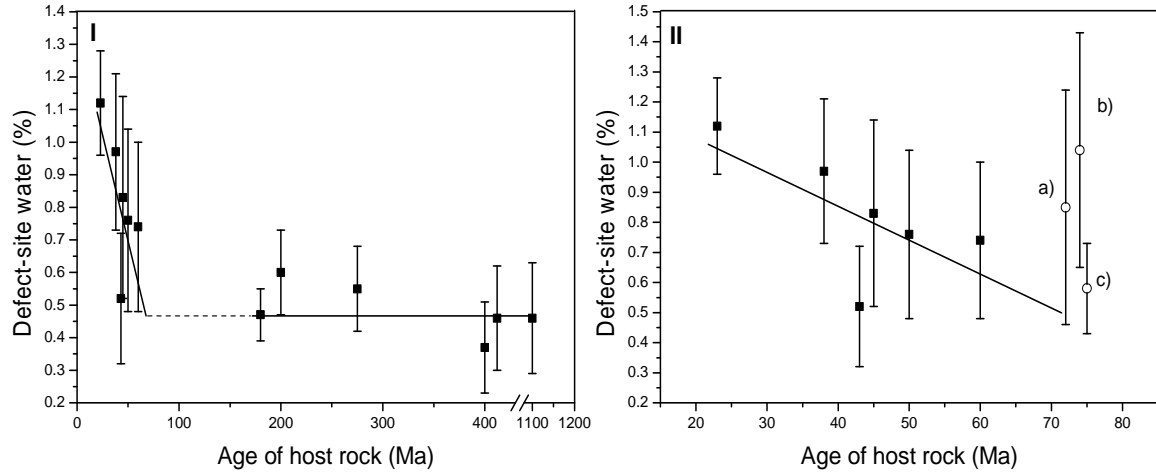


Figure 4. I) Mean defect-site water content of agates from hosts aged from 23 to 1100 Ma. Dashed line is for eye guidance. II) Mean defect-site water content of agates from hosts aged up to 80 Ma. Open circles show a) the overall mean defect-site water content of the Gurasada samples; b) mean defect-site water content of the Gurasada samples with a crystallite size < 60 nm; c) mean defect-site water content of the Gurasada samples with a crystallite size > 60 nm. a) and b) have been off-set slightly from the host age of 75 Ma. Error bars are  $\pm 1$  st. dev.

**Density** New density data has been determined for agates found in Gurasada, Romania; Las Choyas, Mexico and Bay of Fundy, Nova Scotia, Canada; all other density data has been given elsewhere (Moxon et al. 2006).

The collective data of crystallite size, density, moganite and defect-site water content for the individual Gurasada agates are given in Table 3.

Table 3. Data from the individual Gurasada agates

Sample number	$C_{s(101)}$ (nm)	Moganite content (%)	Defect water (%)	Density $g\ cm^{-3}$
High $C_{s(101)}$				
56	67	18	calcite	**nt
59	60	9	0.58	2.628
61	74	10	0.78	2.586
64	78	2	0.43	2.621
65	79	2	0.52	**nt
66	76	4	calcite	2.647
68	64	4	cristobalite	**nt
Mean	71(7)	7(6)	0.58(0.15)	2.621(0.025)
Low $C_{s(101)}$				
51	48	28	1.55	**nt
53	44	19	1.35	2.565
55	44	16	cristobalite	2.621
58	52	8	0.68	2.586
62	44	16	calcite	**nt
63	44	16	1.00	2.599
67	46	19	0.52	2.623
69	41	17	1.12	2.591
71	45	*nt	cristobalite	**nt
75	50	4	cristobalite	**nt
Mean	45(3)	17(9)	1.04(0.39)	2.598(0.022)

\*nt – Measurement not made. The cristobalite content was high and interfered with the Lorentzian fitting.

\*\*nt – Density not taken due to interwoven extraneous material.

## 4 DISCUSSION

### 4.1 Crystallite size and moganite content in agate

Systematic links were shown to exist between the crystallite size of agate and the host rock age in 19 of 22 agate regions (Moxon & Carpenter, 2009). However, agates from three regions produced a crystallite size that suggested agate formation later than the chronological age of the host. Agates from Northumbria, England (host rock age 391 Ma); Rio do Sul, Brazil (133 Ma) and Mt. Somers, New Zealand (89 Ma) were in this category. Isotope evidence and later known volcanic activity were respectively cited to support the claim that agates from Brazil and Northumbria were formed by later volcanic events. Apart from the small crystallite size, no other supporting evidence could be offered for low values found in the New Zealand agates. The crystallite size of the New Zealand and Brazilian agates as a function of age is shown in figure 5 I at points 9 & 10 respectively, and agates from these two regions are regarded as outliers for the rest of this discussion.

The mean crystallite size of agates from eight regions found in hosts  $\leq 60$  Ma exhibit a statistically significant linear growth ( $r = 0.92$ ); the mean standard deviation of the mean crystallite size shown by agates in these regions is  $\pm 9\%$  (Table 2). For agates found in the 50 and 280 Ma age range, there appears to be a cessation of growth that is revealed by the mean of the mean crystallite sizes of agates from five regions found here at 75(4) nm (Fig. 5I). However, this cessation of growth is not due to a lack of moganite as many agates from these hosts have a moganite content  $\geq 5\%$ .

The termination of natural mineral growth is not a new observation and has been shown to occur when a secondary mineral phase exists as a series of discrete particles within a polycrystalline matrix. This phenomenon, known as Zener pinning, has been recognised for over 50 years and is caused by secondary particles creating a restraining force on the developing grain boundary (Nes et al. 1985). In agate, growth does restart at around 280 Ma and continues for the next  $\sim 30$  Ma. At around 310 Ma there is a second cessation of growth that lasts for a further  $\sim 800$  Ma (Moxon & Carpenter, 2009).

The mean crystallite size of the 17 agates from Gurasada produces a standard deviation of  $\pm 25\%$ : this value is much greater than is found in any other agate region from hosts  $\leq 300$  Ma (Table 2). An examination of the Gurasada crystallite size data in Table 3 indicates a natural separation into two

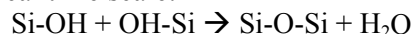
groups with a division of crystallite size  $\sim 60$  nm. The mean size of the high crystallite size Gurasada group is 71(7) nm. This value would be inline with the crystallite size found for agates in other hosts aged 50 to 280 Ma (point c, Fig. 5 II), and supports a claim that these agates in this group were formed around the time of the 75 Ma host rock. However, the low crystallite size group of agates with a mean value of 45(3) nm would suggest a deposition at  $\sim 20$  Ma ago.

The moganite content in agate for a particular region is always more variable than crystallite size (Table 2). However, the mean moganite content (17(9) %) of the designated low crystallite size group of Gurasada agates would suggest a host age  $< 30$  Ma (Table 2). Plots of crystallite size are shown as a function of the moganite content in Fig. 6 I. Here, three representative regions demonstrate the wider spread of moganite content compared to the narrower range of crystallite size. In each case, the data can be encompassed by an approximate ellipse with the moganite content as the major elliptical axis. The moganite content and crystallite size for the full Gurasada data shows a different spread caused by the greater range of the crystallite size data (Table 2, Fig. 6 II dashed line). However, if the Gurasada data is once again divided into the two high and low crystallite size groups,  $<$  and  $> 60$  nm, then similar circumscribing ellipses are produced (a and b in Fig.6 II).

### 4.2 Free and defect-site water in agate

The mean free water in agate has been shown to be independent of the age of the host rock, and values from 11 regions found in host aged 23 to 1100 Ma give free water in the 0.15 to 0.4 % range (Moxon & Ríos, 2004). The overall mean free water for the 10 Gurasada agates is within this range at 0.17(0.07) %. Cristobalite contains a high water content and any Gurasada agates with additional cristobalite have not been investigated.

The age-related loss of defect-site water has been previously demonstrated using thermogravimetry and cathodoluminescence (Moxon & Reed, 2006). It is most likely that this water loss is due to a condensation reaction when neighbouring silanol groups release water over the geological time scale:



The free water plays an important role in dissolving the more soluble moganite that later recrystallises as  $\alpha$ -quartz. As the mean free water is independent of age, then any freshly generated free water must eventually leave the agate.

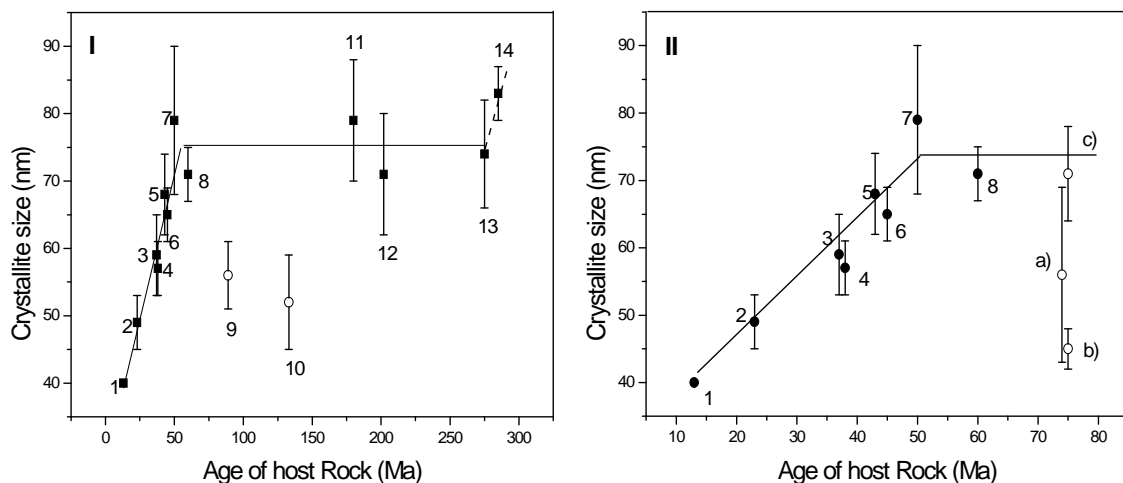


Figure 5 I Crystallite size as a function of age showing agate regions aged up to 300 Ma. The plot shows the initial linear development of crystallite size for the first 60 Ma. Over the next ~ 200 Ma, growth appears to have stagnated. Agates from New Zealand (9) and Brazil (10) are regarded as outliers: see text. Error bars are  $\pm 1$  st. dev. After Moxon & Carpenter (2009).

II Crystallite size as a function of age showing agate regions aged up to 80 Ma. Open circles show the Gurasada data with a) the mean crystallite size of all 17 samples tested; b) the mean crystallite size of the Gurasada agates < 60 nm; c) the mean crystallite size of the Gurasada agates > 60 nm. a) has been off-set slightly from the host rock age of 75 Ma. Error bars are  $\pm 1$  st. dev. Numbers correspond to those in Table 2.

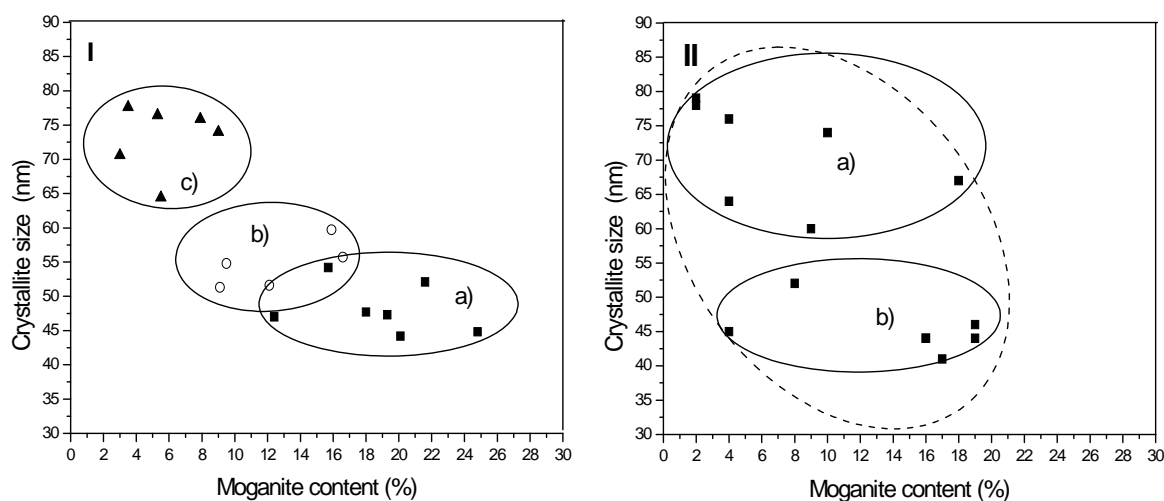


Figure 6 Crystallite size as a function of moganite content. I) Representative agate groups with a crystallite size < 80 nm from a) Mt Warning, Australia (23 Ma)- solid squares; b) Mt. Somers, New Zealand (89 Ma)- open circles; c) Agate Creek, Australia (275 Ma)- solid triangles. II) Agates from Gurasada, Romania showing the proposed division between agates with crystallite size a) > 60 nm and b) < 60 nm respectively. Dashed perimeter encompasses all the Gurasada data.

The mean standard deviation for the defect-site water found in agates from six regions investigated in the 23 to 60 Ma age range is  $\pm 31\%$ . This high standard deviation demonstrates the wide variation of defect-site water in a collection of agates from any particular region. Nevertheless, the mean defect-site water as a function of the host rock age does produce a statistically significant linear relationship for hosts  $\leq 60$

Ma ( $r = 0.7$ ). Inclusion of the full Gurasada data shows that the mean value of the 10 samples is well off trend (point a) in Fig. 4 II. Once again however, a different picture emerges if the defect-site water data of the Gurasada agates is re-considered using the same two groups of agates that produced the low and high crystallite size (points b and c respectively in Fig. 4 II). The mean defect-site water data from the high



crystallite size agates [0.58(15)] now shows a better fit and is in line with the determined 75 Ma Gurasada host rock age, (point c, Fig.4 II). The mean defect-site data from the agates in the low crystallite size group (point b, Fig. 4II) at 1.04(0.39) % is close to the 1.12(0.16) % that was found in chalcedony from the 23 Ma host from Mt. Warning, Queensland, Australia.

#### 4.3 Density variation in agate

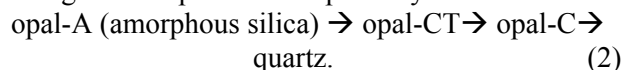
Water mobility over the geological time-scale converts the more soluble and lower density moganite ( $2.55 \text{ g cm}^{-3}$ ; Miehe & Graetsch, 1992) into higher density chalcedony ( $2.57 \rightarrow 2.62 \text{ g cm}^{-3}$ ; Fig. 7). The maximum mean density of  $\sim 2.62 \text{ g cm}^{-3}$  is reached once agates achieve a mean crystallite size of  $\sim 75 \text{ nm}$  (Fig.7). The high crystallite size Gurasada agates have achieved this size, and the density data that is now presented suggests that the maximum agate density is reached around 75 Ma and not the 180 Ma given in Moxon (2009).

Agates from hosts that have been heated by later thermal events have a crystallite size around five times greater than the youngest agate detailed here. It would be anticipated therefore, that an increase in crystallite size would lead to a corresponding increase in density. However, the developing crystallites result in a poor mutual orientation. Hence, the effect of crystallite growth is negated by increasing disorder. Further confirmation of the differences between the two Gurasada groups of agates is shown by the density determinations at points a and b in Fig. 7 for the respective low and high crystallite size samples.

#### 4.4 Cristobalite in the Gurasada agates and possible genesis

One final factor that is different with the Gurasada agates compared to agates from 26 other regions is the identification of strong opal-C signals (the low temperature silica polymorph of cristobalite). A number of the Gurasada agate and chalcedony samples have a white rind on the outer surface (e.g. No. 61a, 53b, 58b, 69b in Fig.2). Using powder XRD, the rind has been identified as a mixture of cristobalite and  $\alpha$ -quartz in varying proportions (Fig.8). In some instances the white deposit is clearly supported in the agate or chalcedony. Additionally, hidden cristobalite has been found in the Gurasada agates; this observation is not new and was found in 8 of 51 samples from agates in hosts  $< 60 \text{ Ma}$  (Moxon & Carpenter, 2009). However, the cristobalite signals in the Gurasada agates are much stronger.

The recognition of hidden cristobalite in agate reveals a possible important indicator for agate genesis as one route for agate formation could be along an amorphous silica pathway:



These particular transformations have been identified as a sequence of stages undergone by silica sinter (Rogers et al. 2004) and chert (Hesse, 1988). For the Gurasada agates, the white cristobalite rind and associated white floaters within the agate have formed contemporaneously with the agate itself. Hidden cristobalite has been found in both the low and high crystallite size groups of agates; hence it is possible that genesis is the result of silica transformations (sequence 2). Unfortunately, it cannot be determined with certainty whether the non-visible cristobalite found in the actual agate structure had its origins from the white rind or formed as a result of changes from an amorphous silica precursor.

The high crystallite size group of agates have demonstrated properties that are in agreement with the radiometrically determined age of the 75 Ma host rock; it is most likely that their formation was linked with the host rock volcanism. Genesis of the low crystallite size group of agates would appear to have had a different silica source however. For these samples, the determined crystallite size and defect-site water indicate an origin around 20 Ma ago. The moganite content and density determinations are less precise but still suggest an origin  $< 30 \text{ Ma}$  ago.

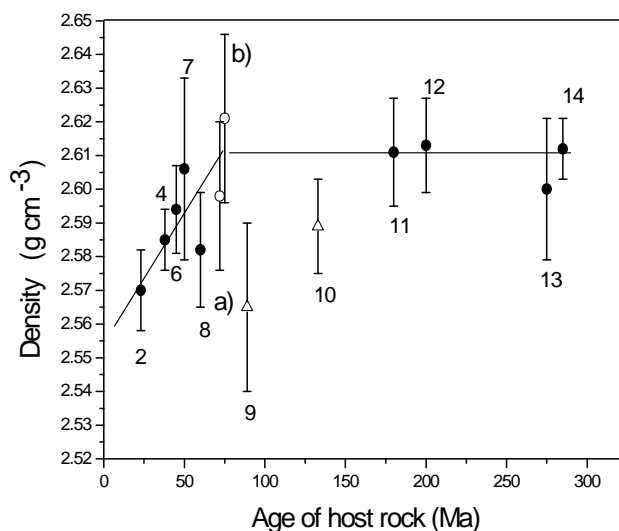


Figure 7 Mean regional density as a function of the age of the host rock. Numbers correspond to those in Table 2. Agates from New Zealand and Brazil (open triangles) are regarded as outliers- see text. The low and high crystallite size agates from Gurasada, Romania (open circles) are shown at a) (slightly off-set) and b) respectively. Error bars are  $\pm 1 \text{ st. dev.}$

Only two periods of volcanic activity have been identified in the Apuseni Mountains: ~ 75 Ma (Constantina et al. 2009) and 9-15 Ma (Roşu et al. 1997; Pécskay et al., 2006). For the present study, a chalcedony vein (sample No. 55) has been found in close association with the altered breccia (Fig. 9). We suggest that a more likely silica source for the younger agates is the extensive alteration (bentonitisation) of the pyroclastic breccia host rock. Such changes release considerable amounts of silica (Meunier, 2005).

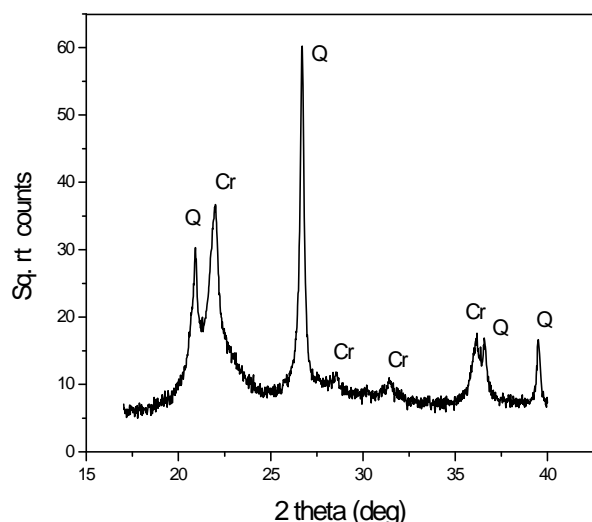


Figure 8 XRD signals from the white material surrounding the agate from sample No. 56. The diffractogram shows good reflections from  $\alpha$ -quartz (Q) and cristobalite (Cr).

## 5. CONCLUSIONS

The origins of agate are unknown, but the links between the mean crystallite size of agates and host rock age indicates that agate formation is generally penecontemporaneous with the creation of the host rock (Fig.5). However, the overall crystallite size, moganite and defect-site water content of the 17 Gurasada agates are consistently well off trend and show a standard deviation greater than any found in 14 other regions from hosts  $\leq 275$  Ma.

The crystallite size division at 60 nm for the Gurasada agates produces two groups defined as high and low crystallite size. There are no obvious distinguishing features in the hand-specimen that would allow a separation into the two groups, but data for the high crystallite size group is consistent with the determined age of the 75 Ma host rock. Furthermore, this is supported by data from density, moganite and defect-site water content. However, the same four properties of the ten Gurasada agates considered as low crystallite size indicate an agate

formation around 55 Ma later. The lack of volcanism in the area and the observed host rock alteration would suggest that the silica source for these later formed agates would be the bentonitisation of the pyroclastic breccia.



Figure 9 A chalcedony vein surrounded by altered breccia.

Good XRD signals of cristobalite can be identified within clear areas in some of the Gurasada agates. Unfortunately, it cannot be demonstrated whether this hidden cristobalite had its origins in the white cristobalite outer rind or whether it formed as a penultimate phase following a series of silica transformations starting with amorphous silica.

## ACKNOWLEDGEMENTS

We are much obliged to the Department of Earth Sciences, Cambridge University, England. Tony Abraham is thanked for his assistance in the X-ray data collection. This agate study has relied upon the generous donation of agate by collectors and research workers from around the world. We are indebted to Rob Burns, Jeannette Carrillo, Nick Crawford, Brad Cross, Gerhard Holzhey, Paul Hoskin, Brian Isfield, Herbert Knuettel, Reg Lacon, Maziar Nazari, Leonid Neymark, John Richmond, Vanessa Tappenden, Bill Taylor.

## REFERENCES

- Bish, D.L. & Reynolds, R.C.Jr., 1989. *Sample preparation for X-ray diffraction* In: *Modern Powder Diffraction* (D.L. Bish and J.E Post, Eds.). Reviews in Mineralogy, **20**, Mineralogical Society of America, Washington D.C. p 73-99.
- Clark, R., 2009. *Fairburn Agate*, Silverwind Agates, Appleton, USA. 130 p.
- Constantina, C., Szakács, A. & Pécskay, Z., 2009. *Petrography, geochemistry and age of volcanic rocks in the Gurasada area, Sothern Apuseni Mts.* Carpathian Journal of Earth and Environmental Sciences, **4**(1), 31-47.
- Daniels, F.J. & Dayvault, R.D., 2006. *Ancient Forests*, Western Colorado Publishing Co., Grand Junction. Colorado, USA. 450 p.
- Deer, W.A., Howie, R.A. & Zussman, J., 1992. *An Introduction to the Rock-Forming Minerals*, Longman, Harlow. UK. 696 p.
- Flörke, O.W., Köhler-Herbertz, B., Langer, K. & Tönges, I., 1982. *Water in microcrystalline quartz of Volcanic Origin: Agates*. Contributions to Mineralogy and Petrology, **80**, 324-333.
- Götze, J., Möckel, R., Kempe, U., Kapitonov, I., & Vennemann, T., 2009. *Characteristics and origin of agates in sedimentary rocks from the Dryhead area, Montana, USA*. Mineralogical Magazine, **73**, 673-690.
- Graetsch, H., Flörke, O.W. & Miehe, G., 1985. *The nature of water in chalcedony and opal-C from Brazilian agate geodes*. Physics and Chemistry of Minerals, **12**, 300-306.
- Heaney, P.J., 1993. *A proposed mechanism for the growth of chalcedony*. Contributions to Mineralogy and Petrology, **115**, 66-74.
- Hesse, R., 1988. *Origin of Chert, 1. Diagenesis of biogenic siliceous sediments*. Geoscience Canada, **15**(3), 171-192.
- Miehe, G. & Graetsch, H., 1992. *Crystal structure of moganite: a new structure type for silica*. European Journal of Mineralogy, **4**, 693-683.
- Moxon, T., 2002. *Agate: a study of ageing*. European Journal of Mineralogy, **14**, 1109-1118.
- Moxon, T. & Ríos, S., 2004. *Moganite and water content as a function of age in agate: an XRD and thermogravimetric study*. European Journal of Mineralogy, **16**, 269-278.
- Moxon, T. & Reed, S.J.B., 2006. *Agate and chalcedony from igneous and sedimentary hosts aged 13 to 3480 Ma: a cathodoluminescence study*. Mineralogical Magazine, **70**, 485-498.
- Moxon, T., Nelson, D.R. & Zhang, M., 2006. *Agate recrystallisation: evidence from samples found in Archaean and Proterozoic host rocks, Western Australia*. Australian Journal of Earth Sciences, **53**, 235-248.
- Moxon, T., 2009. *Studies on Agate*. Terra Publications, Doncaster, UK. 102 p
- Moxon, T. and Carpenter, M.A., 2009. *Crystallite growth kinetics in nanocrystalline quartz (agate and chalcedony)*. Mineralogical Magazine, **73**, 551-568.
- Meunier, A., 2005. *Clays*. Ed. Springer-Verlag Berlin Heidelberg, 472 p.
- Nes, E., Ryum, N. & Hunder, O., 1985. *On the Zener drag*. Acta Metallurgica, **33**(1), 11-22.
- Pécskay, Z., Lexa, J., Szakács, A., Seghedi, I., Balogh K., Konečný, V., Zelenka, T., Kovacs, M., Póka, T., Fülöp, A., Márton, E., Panaiotu, C., Cvetcovič, V., 2006. *Geochronology of Neogene magmatism in the Carpathian arc and intra-Carpathian area*, Geologica Carpathica, **57**(6), 511-530.
- Petrovic, I., Heaney, P.J. & Navrotsky, A., 1996. *Thermochemistry of the new silica polymorph moganite*. Physics and Chemistry of Minerals, **23**, 119-126.
- Rodgers, K.A., Browne, P.R.L., Buddle, T.F., Cook, K.I., Greatrez, R.A., Hampton, W.A., Herdianita, N.R., Holland, G.R., Lynne, B.Y., Martin, R., Newton, Z., Pastars, D., Sannazarro, K.L. and Teece, C.I.A., 2004. *Silica phases in sinters and residues from geothermal fields of New Zealand*. Earth Science Reviews, **66**, 1-61.
- Roşu, E., Pécskay, Z., Ştefan, A., Popescu, G., Panaiotu, G., Panaiotu, C.E. 1997. *The evolution of the Neogene volcanism in the Apuseni Mountains (Rumania): Constraints from new K-Ar data*, Geologica Carpathica, **48**(6), 353-359.
- Yamagishi, H., Nakashima, S. & Ito, Y., 1997. *High temperature infrared spectra of hydrous microcrystalline quartz*. Physics and Chemistry of Minerals, **24**, 66-74.

Received at: 22. 02. 2010

Accepted for publication at: 26. 04. 2010

Published online at: 29. 04. 2010